

Noisy Kondo impurities

T. Delattre^{1,2}, C. Feuillet-Palma^{1,2}, L.G. Herrmann^{1,2}, P. Morfin^{1,2}, J.-M. Berroir^{1,2}, G. Fève^{1,2}, B. Plaçais^{1,2}, D.C. Glattli^{1,2,3}, M.-S. Choi⁴, C. Mora^{1,2} and T. Kontos^{1,2*}

¹*Ecole Normale Supérieure, Laboratoire Pierre Aigrain,
24, rue Lhomond, 75231 Paris Cedex 05, France*

²*CNRS UMR 8551, Laboratoire associé aux universités
Pierre et Marie Curie et Denis Diderot, France*

³*Service de physique de l'état Condensé,
CEA, 91192 Gif-sur-Yvette, France.*

⁴*Department of Physics, Korea University, Seoul 136-713, Korea*

(Dated: September 20, 2018)

arXiv:1010.4815v1 [cond-mat.mes-hall] 22 Oct 2010

* To whom correspondence should be addressed: kontos@lpa.ens.fr

The anti-ferromagnetic coupling of a magnetic impurity carrying a spin with the conduction electrons spins of a host metal is the basic mechanism responsible for the increase of the resistance of an alloy such as $\text{Cu}_{0.998}\text{Fe}_{0.002}$ at low temperature, as originally suggested by Kondo¹. This coupling has emerged as a very generic property of localized electronic states coupled to a continuum²⁻⁷. The possibility to design artificial controllable magnetic impurities in nanoscopic conductors has opened a path to study this many body phenomenon in unusual situations as compared to the initial one and, in particular, in out of equilibrium situations⁸⁻¹⁰. So far, measurements have focused on the average current. Here, we report on *current fluctuations* (noise) measurements in artificial Kondo impurities made in carbon nanotube devices. We find a striking enhancement of the current noise within the Kondo resonance, in contradiction with simple non-interacting theories. Our findings provide a test bench for one of the most important many-body theories of condensed matter in out of equilibrium situations and shed light on the noise properties of highly conductive molecular devices.

The hallmark of the Kondo effect in a quantum dot is an increase of the conductance below T_K up to the unitary conductance $2e^2/h$ at very low temperature and bias voltage. This corresponds to the opening of a spin degenerate conducting channel of transmission 1 at the Fermi energy of the electrodes, if only a single spin 1/2 is involved. The non-interacting theory of shot noise predicts no noise for such a quantum scatterer, as a consequence of Fermi statistics¹¹. Does such a statement apply to a generic Kondo resonance ?

In this letter, we show that, in contrast to the prediction of the non-interacting theory, a conductor in the Kondo regime can be noisy even though its conductance is very close to $2e^2/h$. We report on noise measurements carried out in single wall carbon nanotube based quantum dots in the Kondo regime. We find an enhancement up to an order of magnitude with respect to the non-interacting (Fermi gas) theory of the shot noise within the Kondo resonance due to charge quantization combined with spin and orbital degeneracy. We can account for this enhancement with a fully interacting theory based on the Slave Boson Mean Field technique (SBMF). We also find a non-monotonic variation of the equilibrium current fluctuations as the temperature is decreased below T_K . Finally, the conductance *and* the noise obey a scaling law, the Kondo temperature $k_B T_K$ being the only energy scale.

Single wall carbon nanotubes (SWNTs) are ideally suited to explore the noise in the Kondo regime of a quantum dot. They can exhibit Kondo temperatures up to $10 - 15K$, which allows to apply rather high currents, up to $10nA$, *within* the Kondo resonance. This contrasts with semiconducting quantum dots where Kondo temperatures are usually much smaller and therefore shot noise measurements more difficult (a specific aspect of the spin $1/2$ case could be studied only very recently in a lateral quantum dot¹²). In addition, carbon nanotubes allow to investigate a large class of different Kondo effects, including the simplest spin $1/2$ Kondo effect⁵, the 2-particle Kondo effect¹³, the orbital Kondo effect¹⁴ and the so-called SU(4) Kondo effect^{14,15}.

We first present results for device A which consists of a SWNT contacted by two Pd electrodes separated by $200nm$ (see figure 1b). Our measurement setup, shown on figure 1b, allows to measure simultaneously the noise and the conductance. The *total current noise* S_I of the SWNT is obtained by subtracting a calibrated offset to the measured cross-correlations (see Methods and Supplementary information). The color scale plot of the differential conductance of the sample is displayed on figure 1a and the characteristic Kondo ridges are observed at $1.4K$ as the horizontal lines within the Coulomb diamonds. We now study the two ridges, Sample A Ridge 1 (SAR1) and Sample A Ridge 2 (SAR2), corresponding to the gate voltage $V_G = 11.26V$ and $V_G = 11.80V$ respectively, indicated by an arrow in figure 1a.

Signatures of the Kondo effect are already present in the equilibrium current fluctuations. From the fluctuation-dissipation theorem, the power spectral density of current noise is expected to be given by the Johnson-Nyquist formula : $S_I(V_{sd} = 0) = 4k_B T G(T, V_{sd} = 0)$, where $G(T, V_{sd}) = dI/dV$ is the differential conductance at temperature T and source-drain bias V_{sd} . However, due to Kondo correlations, $G(T, V_{sd} = 0)$ displays a sharp increase as T is lowered, as shown on figure 1c left inset, in blue dashed lines. From the Johnson-Nyquist formula, an increase of $G(T, V_{sd} = 0)$ tends to produce an increase of S_I as the temperature is lowered but at zero temperature, S_I should be zero. Therefore, an unusual maximum can occur in the variation of S_I as a function of temperature for a quantum dot in the Kondo regime. We observe such a maximum around $3K$ for ridge SAR1, as shown in the left inset of figure 1c in black squares, which reaches about 7 to $9 \times 10^{-27} A^2/Hz$ here. As expected, the Johnson-Nyquist relationship still holds, as shown in the right inset of figure 1c.

The bias dependence of $G(1.4K, V_{sd})$ for SAR1 and SAR2 is displayed on figure 2. The

characteristic zero bias peak of the Kondo effect is observed. The conductance at zero bias is, for both cases, close to $2e^2/h$ (respectively $0.997 \times 2e^2/h$ and $0.865 \times 2e^2/h$). The half-width of these resonances, of about $0.2meV$, gives an estimate of the Kondo temperature, of about $2.5K$, consistent with the temperature dependence shown in figure 1c left inset. As shown on figure 2a and b (black squares), when a finite bias is applied, the *total* noise power spectral density S_I increases from about $5 \times 10^{-27} A^2/Hz$ to about $8 \times 10^{-27} A^2/Hz$ ($7 \times 10^{-27} A^2/Hz$) for SAR1(SAR2) respectively. The ratio of S_I to the Schottky value $2eI_{sd}$, where I_{sd} is the current flowing through the nanotube at $V_{sd} = 0.84mV$, is about 0.84 ± 0.09 (0.89 ± 0.1) for SAR1(SAR2) respectively. Therefore, the noise remains sub-poissonian.

In general, the noise properties of carbon nanotubes are affected by the existence of a possible orbital degeneracy, which arises from the band structure of graphene, as recently shown in the non-interacting limit¹⁶. Therefore, a first step towards the understanding of the measurements presented in figure 2 is to use a resonant tunneling model with *two spin degenerate channels*, with transmission $\tilde{D}_{i,res}(\epsilon) = d_i/(1 + \epsilon^2/\Gamma^2)$, d_i being the transmissions of the channel of index $i \in \{1, 2\}$ and Γ being the width of the resonant level and ϵ being the energy. From the non-interacting scattering theory¹¹, the current and the noise associated with $\tilde{D}_{i,res}$ read:

$$I(V_{sd}) = \frac{2e}{h} \sum_{i=1,2} \int_{-\infty}^{\infty} \tilde{D}_{i,res}(\epsilon)(f_L - f_R)d\epsilon \quad (1)$$

$$S_I(V_{sd}) = \frac{4e^2}{h} \sum_{i=1,2} \int d\epsilon \{ \tilde{D}_{i,res}(\epsilon)[f_L(1 - f_L) + f_R(1 - f_R)] + \tilde{D}_{i,res}(\epsilon)[1 - \tilde{D}_{i,res}(\epsilon)](f_L - f_R)^2 \} \quad (2)$$

with $f_L = f(eV_{sd}/2 + \epsilon)$ and $f_R = f(-eV_{sd}/2 + \epsilon)$, $f(\epsilon)$ being the Fermi function at temperature T . The fits of dI/dV using equation (1) and $\tilde{D}_{i,res}$, shown in blue dashed lines in figure 2, panel a.(b.), yield $d_1 = d_2 = 0.95$ ($d_1 = d_2 = 0.99$) and $\Gamma = 0.11meV$ ($\Gamma = 0.09meV$) respectively. These fits are poor because the Lorentzian line shape with constant Γ assumed for $\tilde{D}_{i,res}$ is not able to account for both the height and the width of the measured dependence of dI/dV as a function of V_{sd} . Furthermore, the noise obtained with formula (2) using the above values for d_1 , d_2 and Γ , in blue dashed lines in the lower panels of figure 2, is about an order of magnitude smaller than our experimental findings. Therefore, a simple non-interacting resonant tunneling theory can account neither for the conductance nor for the noise that we observe.

In the Kondo regime, in case of a fourfold degeneracy and single charge occupancy, the maximum of the resonance lies at T_K above the Fermi energy of the leads according to the Friedel sum rule, as depicted on figure 3b. From this, one can infer that, if the couplings of the level to the left Γ_L and the right Γ_R electrodes are the same (hereafter called the symmetric case), the differential conductance which saturates at $2e^2/h$ corresponds to *two channels of transmission 1/2* ($\frac{1}{2} \times \frac{4\Gamma_L\Gamma_R}{(\Gamma_L+\Gamma_R)^2}$ in the general case). This corresponds to the so-called SU(4) Kondo effect where the spin *and* the orbital degree of freedom play an equivalent role^{18,19} in the Kondo screening.

Unfortunately, no full out-of-equilibrium theory of the Kondo effect is available. As shown below, our experiments are carried out in a regime where $T \sim T_K/3$ and $eV_{sd} \lesssim 3k_B T_K$. Therefore, one has to choose a low energy theory in order to understand our experiment. Essentially 3 different approaches can be used : the Fermi Liquid (FL) theory, the Slave Boson Mean Field (SBMF) theory and the Non-Crossing Approximation (NCA)²⁰. Both SBMF and FL theory are expected to be exact in the zero-energy limit ($k_B T = eV_{sd} = 0$). Presently available FL theories²¹⁻²⁴ provide the correct description only at very low energies and give unphysical results for the temperature and bias range of our experiment. On the other hand, the SBMF theory turns out to be more robust up to the energy range of our experiment²⁰. The NCA is a good approximation at relatively higher energies, and becomes inaccurate at temperatures much smaller than T_K . It gives results similar to the SBMFT at energies not too small compared with T_K ²⁰. Therefore, we use a SBMF approach which is the simplest one available. In order to account for the orbital degeneracy, we use a SU(4) theory. Such a model should be regarded as the minimal one to explain our data and one should bear in mind that our samples might be in a regime where the full fourfold degeneracy is only approximately fulfilled. The SBMF has been widely used in the spin degenerate (SU(2)) case to compute the noise in quantum dots in the Kondo regime²⁵ and in the SU(4) case to study the conductance¹⁸. We generalize here this approach for the noise. In the SBMF approach, one still uses formulae (1) and (2) replacing $\tilde{D}_{i,res}(\epsilon)$ by $\tilde{D}_{SBMF}(\epsilon, V_{sd})$ which accounts for the interactions in a self-consistent way. It is a Breit-Wigner formula with a level position $\tilde{\epsilon}_0$ and a width $\tilde{\Gamma}$ which explicitly depend on V_{sd} and T . In the SU(4) limit, one has in the symmetric case:

$$\tilde{D}_{SBMF}(\epsilon, V_{sd}, T) = \frac{\tilde{\Gamma}^2}{\left(\frac{\epsilon}{k_B T_K} - \tilde{\epsilon}_0\right)^2 + \tilde{\Gamma}^2} \quad (3)$$

with $\tilde{\Gamma}^2 \approx -\frac{t^2}{6} - \frac{x^2}{8} + \sqrt{1 + (\frac{t^2}{6} + \frac{x^2}{8})^2}$ and $\tilde{\epsilon}_0^2 \approx \frac{t^2}{6} + \frac{x^2}{8} + \sqrt{1 + (\frac{t^2}{6} + \frac{x^2}{8})^2}$, where $x = eV_{sd}/k_B T_K$, $t = \pi T/T_K$.

From formula (3), $\tilde{D}_{SBMF}(\epsilon = 0, V_{sd} = 0, T = 0) = 1/2$. This contrasts with the general expression of $\tilde{D}_{i,res}(\epsilon)$ for which the transmission at zero energy can take any value between 0 and 1. In addition, $\tilde{\epsilon}_0$ and $\tilde{\Gamma}$ are universal functions of $x = eV_{sd}/k_B T_K$ and $t = \pi T/T_K$. Both facts originate from electron-electron interactions. From equations (1) and (3), the conductance is fitted with *only one* parameter, $k_B T_K$. The outcome of the combination of equations (1), (2) and (3) is shown as solid red lines in figure 2a and figure 2b for $k_B T_K = 0.305 meV$ and $k_B T_K = 0.26 meV$ respectively. We find a good agreement with the experimental data using this SU(4) theory. The agreement is quantitative for the noise of SAR1 and the conductance of SAR2. The conductance of SAR1 peaks at a higher value than the one predicted by the SBMF, although the theoretical line corresponds to the fully symmetric case. This is probably due to the fact that the sample is not far from the mixed valence regime²⁷ for SAR1. Indeed, as can be seen on the linear conductance curve of figure 1a., the single charge peaks slightly overlap at $V_G = 11.26V$. The noise of SAR2 is close to the theoretical curve in the (most important) out of equilibrium regime i.e. $|V_{sd}| > 0.2 meV$. For low bias, a spurious shift less than 10% of the total noise, of about $0.4 \times 10^{-27} A^2/Hz$, occurs. It probably originates from a systematic background variation for $V_G = 11.80V$. Overall, the SBMF SU(4) theory is in much better agreement than the non-interacting resonant tunneling theory. Both the conductance *and* the noise data are accounted for by a *single* energy scale, $k_B T_K$, even though the two actual Kondo impurities have Kondo temperatures differing by about 15%.

A scaling behavior is a well-known property of the Kondo effect²⁷. It has been tested only very recently in a lateral quantum dot, for the bias dependence of the conductance in the SU(2) case¹⁰. We have studied 4 ridges in device A and 1 in device B. For the 5 different Kondo ridges studied, we observe a scaling of $G(T, 0)$ versus T/T_K and of $G(1.4, V_{sd})$ versus $eV_{sd}/k_B T_K$, as shown on figure 4a and b. For the temperature and bias dependences, the data is very well accounted for by the empirical formulae $G = C_0/(1+(2^{1/s}-1)(T/T_K)^2)^{s10,17}$ with $s = 1.02 \pm 0.04$ and $G = G(1.4K, 0) \times \exp[-2(\frac{eV_{sd}}{2.3k_B T_K})^2]$ respectively. Independently of the low energy theory, a similar behavior is expected for the noise²⁰⁻²⁴ because scaling is an essential feature of Kondo physics, linked to the fact that there is only one

energy scale, T_K which controls the electronic system. We introduce $I_0 = \frac{2e^2}{h} \times 2D_0V_{sd}$ and $S_0 = \frac{4e^2}{h}(4k_BTD_0^2 + 2eD_0(1 - D_0)V_{sd} \coth(\frac{eV_{sd}}{2k_B T}))$ which are the zeroth order for the current and the noise for $T/T_K, eV_{sd}/k_B T_K \rightarrow 0$ in the theory. For each Kondo ridge, the parameters D_0 ($D_0 = \frac{h}{4e^2}G(T = 0, V_{sd} = 0) = 2\frac{\Gamma_L\Gamma_R}{(\Gamma_L + \Gamma_R)^2}$) and T_K are obtained from the fitting of the conductance with the SBMF theory. We get the corresponding sets {Sample, Gate voltage, $k_B T_K/e, 2D_0$ } as {A, 11.80V, 0.26mV, 1}, {A, 9.67V, 0.181mV, 0.94}, {A, 17.65V, 0.26mV, 0.58}, {A, 11.26V, 0.305mV, 1} and {B, 3.025V, 0.29mV, 0.99}. In order to test the scaling of the noise, we study $\delta S = S_{exc,0} - S_{exc,I}$ as a function of $\delta I = I_0 - I$ as displayed on figure 4c, $S_{exc,(0,I)}$ being the excess noise defined as $S_{exc,(0,I)} = S_{(0,I)}(V_{sd}) - S_{(0,I)}(V_{sd} = 0)$. We observe the same behaviour for all the 5 ridges which can be fitted as $\delta S = (0.45 \pm 0.05) \times 2e\delta I + 0.2 \pm 0.2$. The value of the slope is the central *quantitative* result of this letter. It is close to 1/2 which is the number predicted by the SBMF theory. For the symmetric case, this value is exact at $T = 0$ and is a very good approximation up to $T = T_K/2$ (see Supplementary information). Even though T_K and/or D_0 can vary by as much as 40%, the noise properties of the Kondo impurity remain invariant.

METHODS

Experimental

Our SWNTs are grown by chemical vapor deposition. They are localized with respect to alignment markers with an atomic force microscope (AFM) or a scanning electron microscope (SEM). The contacts are made by e-beam lithography followed by evaporation of a 70nm-thick Pd layer at a pressure of $10^{-8}mbar$. The highly doped Si substrate (resistivity of $4 - 8m\Omega.cm$) covered with 500nm SiO_2 is used as a back-gate at low temperatures. The typical spacing between the Pd electrodes is between 200nm and 500nm. The current fluctuations in the NT result in voltage fluctuations along the two resistors (of 200Ω) shown in figure 1b. The two signals are fed into two coaxial lines and separately amplified at room temperature by two independent sets of low noise amplification stages (gains: $G_1 = 7268 \pm 10$, $G_2 = 7304 \pm 10$, amplifiers NF SA-220F5). We calculate the cross correlation spectrum with a spectrum analyzer. Each noise point corresponds to 20 averaging runs of 40000 spectra with a frequency span of 78.125kHz (1601 frequency points) and a center frequency of 1.120MHz or 2.120MHz. The sensitivity is about $3 \times 10^{-28}A^2/Hz$. The raw data are corrected by an offset amounting to $(4.2(\pm 0.1) + 19.5(\pm 0.2)\frac{h}{4e^2}G(T, V_{sd}))10^{-27}A^2/Hz$ which is in very good agreement with the circuit diagram of our measurement setup (see Supple-

mentary information).

Fitting details

Throughout the paper, a SU(4) SBMF theory is used (as a minimal model). However, the SU(2) SBMF theory does not account for the data (see supplementary information). When fitting with the SBMF, we have interpolated the low bias expression of $\tilde{\Gamma}$ with a V_{sd} -independent expression for $|V_{sd}| > 0.7\text{meV}$, $\tilde{\epsilon}_0$ remaining unchanged. Such an interpolation has been widely used (see e.g.²⁶) in order to cope with the well-known phase transition problem of the SBMF approach at high bias (see Supplementary information). Finally, when fitting the temperature dependence of the conductance for all the 5 ridges studied with the empirical formula described in the main section, we have found a s parameter larger than that usually found in the literature except for the experiment in reference 17, where the SU(4) case was considered for the first time. Note however that it is distinct from the non-interacting resonant tunneling model which would lead to $1/T$ dependence for large T .

Correspondence. Correspondence and requests for materials should be addressed to T.K. : kontos@lpa.ens.fr

Acknowledgements. We thank A. Cottet for a critical reading of the manuscript and K. LeHur, P. Simon, L. Glazman and N. Regnault for illuminating discussions. This work is supported by the SRC (R11-2000-071) contract, the BK21 contract, the ANR-05-NANO-055 contract, the EU contract FP6-IST-021285-2 and by the C’Nano Ile de France contract SPINMOL.

Competing financial interests. The authors declare no competing financial interests.

-
- ¹ Kondo, J. Resistance Minimum in Dilute Magnetic Alloys. *Prog. Theor. Phys.***32**, 37 (1964)
 - ² Li, J., Schneider, W.-D., Berndt, R. and Delley, B. Kondo Scattering Observed at a Single Magnetic Impurity. *Phys. Rev. Lett.* **80**, 2893 (1998).
 - ³ Madhavan, V., Chen, W., Jamneala, T., Crommie, M.F. and Wingreen, N.S. Tunneling into a Single Magnetic Atom: Spectroscopic Evidence of the Kondo Resonance. *Science* **280**, 567 (1998).
 - ⁴ Goldhaber-Gordon, D., Shtrikman, H., Mahalu, D., Abusch-Magder, D., Meirav, U. and Kastner, M. A. Kondo effect in a single-electron transistor. *Nature* **391**, 156 (1998).
 - ⁵ Nygard, J., Cobden, D.H. and Lindelof, P.E. Kondo physics in carbon nanotubes. *Nature* **408**,

- 342 (2000).
- ⁶ Park, J. et al. Coulomb blockade and the Kondo effect in single-atom transistors. *Nature* **417**, 722 (2002).
- ⁷ Liang, W., Shores, M.P., Bockrath, M., Long, J.R. and Park, H. Kondo resonance in a single-molecule transistor. *Nature* **417**, 725 (2002).
- ⁸ De Franceschi, S. et al. Kondo effect out of equilibrium in a mesoscopic device. *Phys. Rev. Lett.* **89**, 156801 (2002).
- ⁹ Paaske, J., Rosch, A., Wölfle, P. Non-equilibrium singlet-triplet Kondo effect in carbon nanotubes. *Nature Phys.* **2**, 460 (2006).
- ¹⁰ Grobis, M., Rau, I.G., Potok, R.M., Shtrikman, H. and Goldhaber-Gordon, D. Universal Scaling in Nonequilibrium Transport through a Single Channel Kondo Dot. *Phys. Rev. Lett.* **100**, 246601 (2008).
- ¹¹ Blanter, Ya. M., and Büttiker, M. Shot Noise in Mesoscopic Conductors. *Phys. Rep.* **336**, 1 (2000).
- ¹² Zarchin, O., Zaffalon, M., Heiblum, M., Mahalu, D., and Umansky, V. Two-electron bunching in transport through a quantum dot induced by Kondo correlations. *Phys. Rev. B* **77**, 241303 (2008).
- ¹³ Babic, B., Kontos, T. and Schönenberger, C. On the Kondo effect at half filling. *Phys. Rev. B* **70**, 195408 (2004).
- ¹⁴ Jarillo-Herrero, P., Kong, J., van der Zant, H.S.J., Dekker, C., Kouwenhoven, L. P. and De Franceschi, S. Orbital Kondo effect in carbon nanotubes. *Nature* **434**, 484 (2005).
- ¹⁵ Makarovski, A., Liu, J. and Finkelstein, G. Evolution of Transport Regimes in Carbon Nanotube Quantum Dots. *Phys. Rev. Lett.* **99**, 066801(2007).
- ¹⁶ Herrmann, L.G., al. Shot Noise in Fabry-Perot Interferometers Based on Carbon Nanotubes. *Phys. Rev. Lett.* **99**, 156804 (2007).
- ¹⁷ Sasaki, S., Amaha, S., Asakawa, N., Eto, M. and Tarucha, S. Enhanced Kondo Effect via Tuned Orbital Degeneracy in a Spin 1/2 Artificial Atom. *Phys. Rev. Lett.* **93**, 017205 (2004).
- ¹⁸ Lim, J.S., Choi, M.-S., Choi, M.Y., López, R. and Aguado R. Kondo effects in carbon nanotubes: From SU(4) to SU(2) symmetry. *Phys. Rev. B* **74**, 205119 (2006).
- ¹⁹ Le Hur, K., Simon, P. and Loss, D. Transport through a quantum dot with SU(4) Kondo entanglement. *Phys. Rev. B* **75**, 035332 (2007).

- ²⁰ Meir, Y., and Golub, A. Shot Noise through a Quantum Dot in the Kondo Regime. *Phys. Rev. Lett.* **88**, 116802 (2002).
- ²¹ Gogolin, A.O. and Komnik, A. Full Counting Statistics for the Kondo Dot in the Unitary Limit. *Phys. Rev. Lett.* **97**, 016602 (2005).
- ²² Sela, E., Oreg, Y., von Oppen, F. and Koch, J. Fractional Shot Noise in the Kondo Regime. *Phys. Rev. Lett.* **97**, 086601(2006).
- ²³ Mora, C., Leyronas, X. and Regnault, N. Current Noise through a Kondo Quantum Dot in a SU(N) Fermi Liquid State. *Phys. Rev. Lett.* **100**, 036604 (2008).
- ²⁴ Vitushinsky, P., Clerk, A.A., and Le Hur, K. Effects of Fermi Liquid Interactions on the Shot Noise of an SU(N) Kondo Quantum Dot. *Phys. Rev. Lett.* **100**, 036603 (2008).
- ²⁵ Lopez, R. and Sanchez, D. Nonequilibrium Spintronic Transport through an Artificial Kondo Impurity: Conductance, Magnetoresistance, and Shot Noise. *Phys. Rev. Lett.* **90**, 116602 (2004).
- ²⁶ Lopez, R., Aguado, R. and Platero, G. Shot noise in strongly correlated double quantum dots. *Phys. Rev. B* **69**, 235305 (2004).
- ²⁷ Haldane, F.D.M. Scaling Theory of the Asymmetric Anderson Model. *Phys. Rev. Lett.* **40**, 416 (1978).

FIG. 1: Anomalous temperature dependence of the current noise at the onset of the Kondo effect.

a. Colorscale plot of the differential conductance as a function of the gate voltage V_G and the source-drain bias V_{sd} at $T = 1.4K$. The characteristic horizontal lines in the middle of the Coulomb diamonds signaling the Kondo effect are observed. In green lines, the linear conductance curves at $T = 1.4K$ (solid line) and $T = 12K$ (dashed line). b. Simplified diagram of the noise measurement scheme and SEM picture of a typical sample. The bar corresponds to $1\mu m$. c. In the left inset, the non-monotonic temperature dependence of the equilibrium current fluctuations on the Kondo ridge SAR1 ($V_G = 11.26V$ (black squares)). In blue circles, the corresponding variation of $G(T, V_{sd} = 0)$. In solid black line, the predicted dependence of S_I from the Johnson-Nyquist formula. In the right inset, S_I is plotted versus $4k_B T G(T, V_{sd} = 0)$. The line corresponds to the expected slope of 1. The error bars correspond to the mean square root of the statistical error and the systematic error due to fluctuations of the background.

FIG. 2: Noise enhancement within the Kondo resonance.

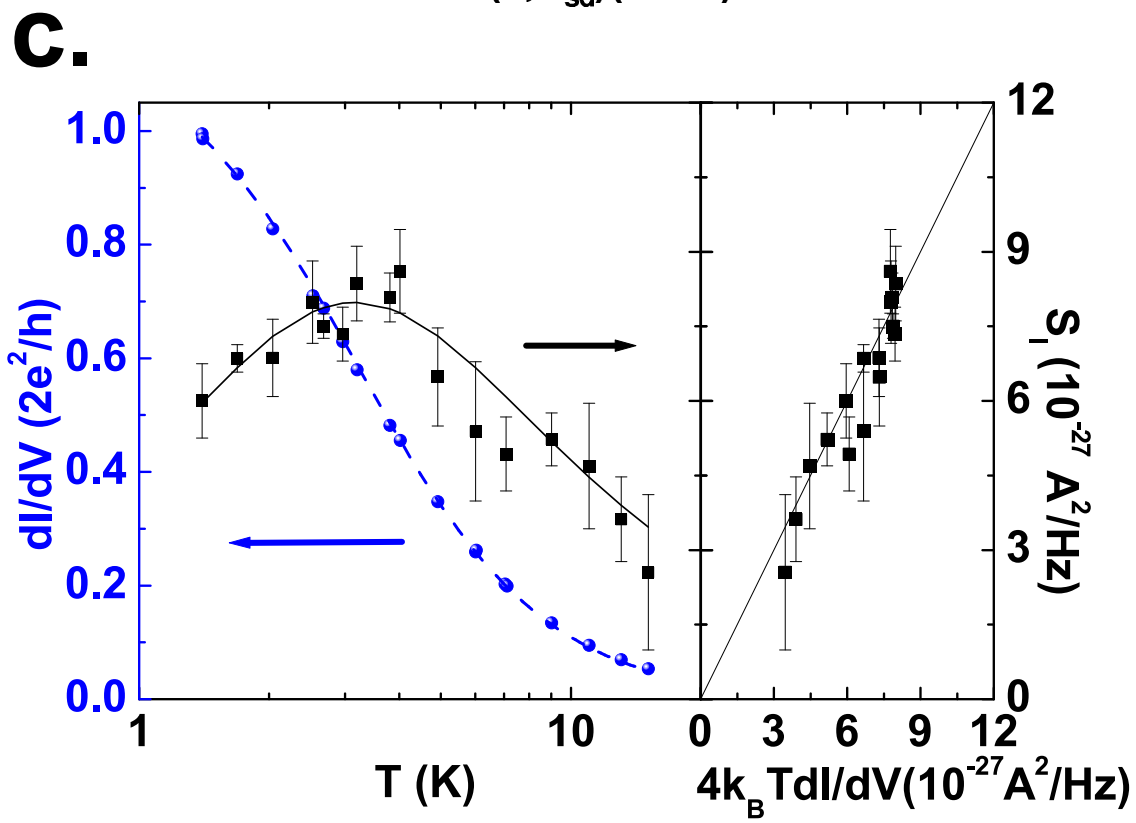
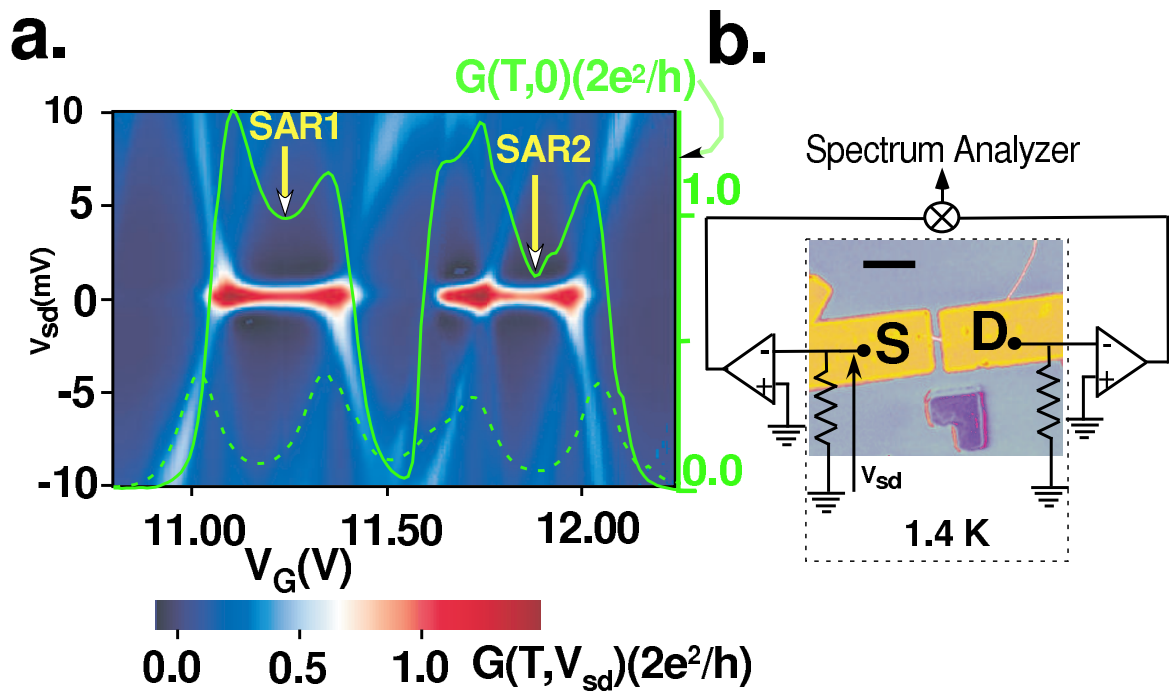
a. Conductance and noise measurements (black circles and black squares respectively) for the Kondo ridge 1 of Sample A ($V_G = 11.26V$) at $1.4K$. The results of the SBMF theory, in solid red lines, are in good agreement with the conductance and the noise. b. Similar plots as in panel a. for the Kondo ridge 2 of sample A ($V_G = 11.80V$). The Kondo resonance corresponds to a slightly different Kondo temperature. In both panels, the non-interacting theory, in blue dashed lines, accounts neither for the conductance nor for the noise. The error bars correspond to the mean square root of the statistical error and the systematic error due to fluctuations of the background.

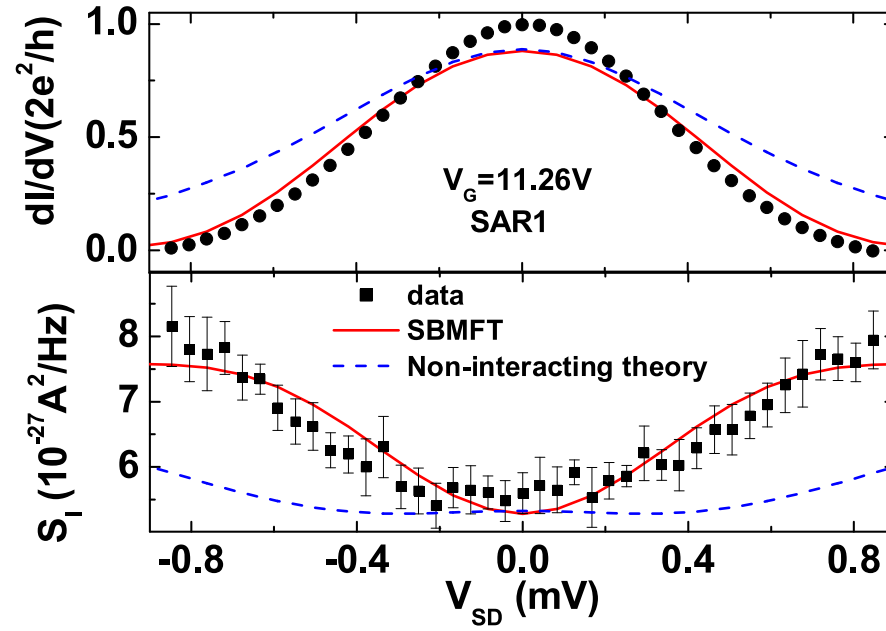
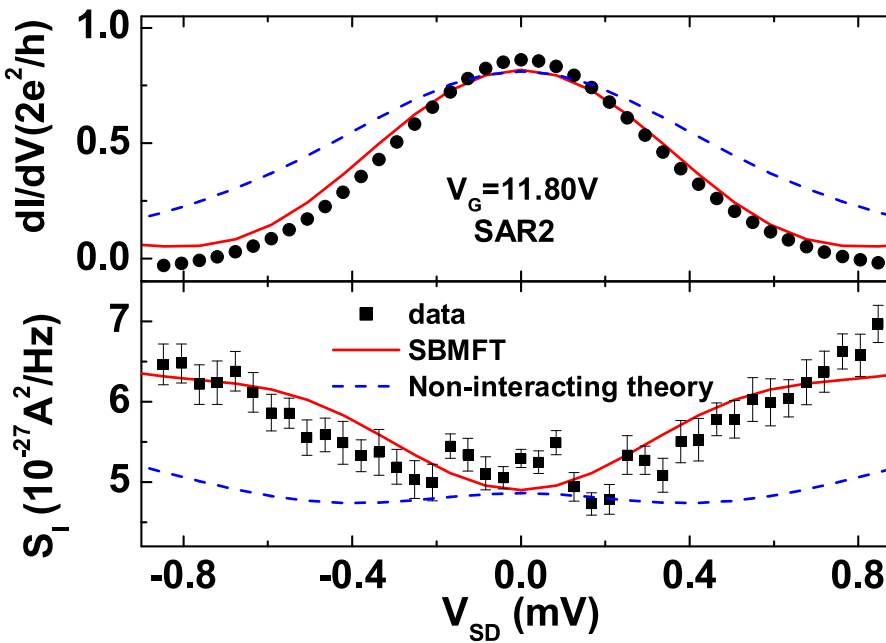
FIG. 3: Schematics of the two limiting cases for noise in a single wall carbon nanotube in the Kondo regime.

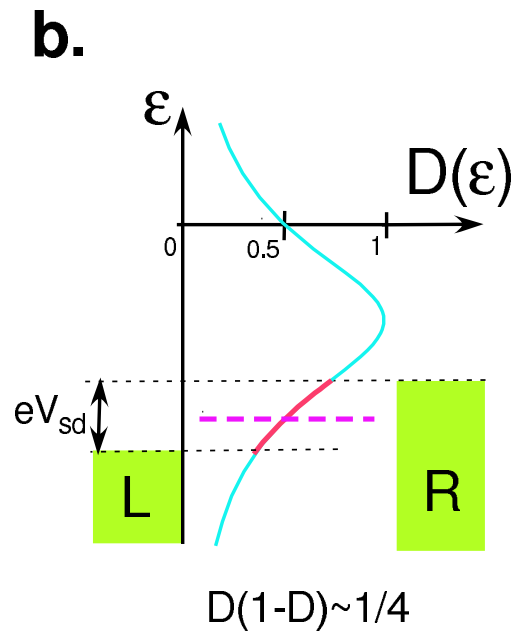
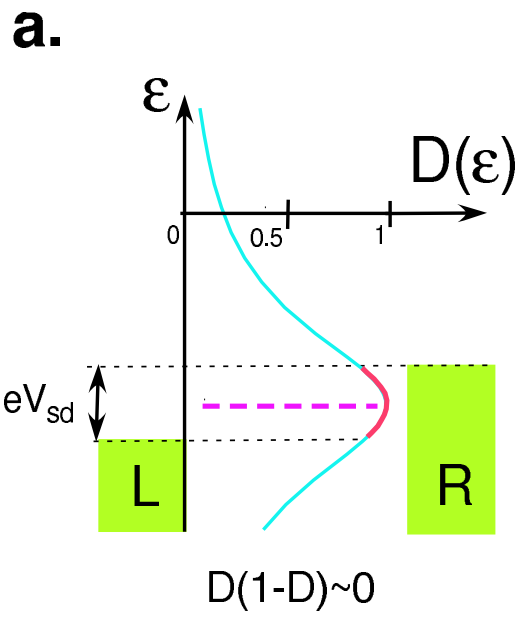
The blue line depicts the line shape of the energy dependent transmission of the Kondo resonance. The red line depicts the part of the transmission accessible in the "transport window" eV_{sd} . The rose dashed line is the position of the Fermi level of the reservoirs for $V_{sd} = 0$. a. For the twofold degenerate case, the effective transmission per channel is close to 1 and only one channel contributes to transport, leading to a suppression of the shot noise ($D(1 - D)$ close to 0). b. For the fourfold degenerate case, the effective transmission per channel is close to 1/2 and there are two channels, leading to an enhancement of the shot noise ($D(1 - D)$ close to 1/4).

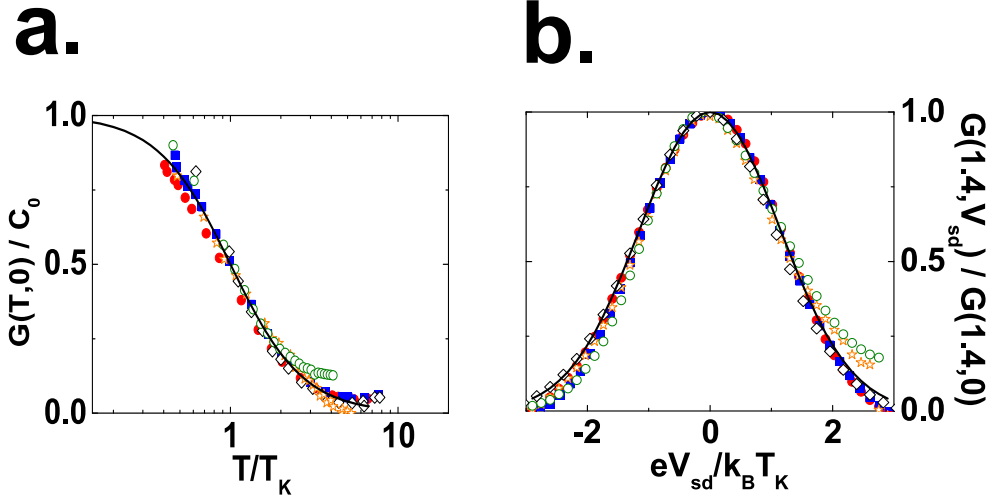
FIG. 4: Scaling properties of the noise of the Kondo 'impurities'.

a. Scaling of the temperature dependence of the zero bias conductance. b. Scaling of the bias dependence of the conductance at $1.4K$. For the temperature (panel a.) and bias dependence (panel b.), the data is very well accounted for by the empirical formulae $G = C_0 / (1 + (2^{1/s} - 1)(T/T_K)^2)^s$ with $s = 1.02$ and $G = G(1.4K, 0) \times \exp[-2(\frac{eV_{sd}}{2.3k_B T_K})^2]$ respectively (in solid lines). c. Scaling of the noise for the different 'Kondo impurities' measured. The line corresponds to the slope of 1/2 predicted by the SBMF. Inset: the different symbols used in the figure and their corresponding 'Kondo impurity'.



a.**b.**





c.

